An explicit nonstandard finite difference scheme for the FitzHugh-Nagumo equations

R. Appadu, M. Chapwanya *, O. A. Jejeniwa, and J.M-S. Lubuma

Department of Mathematics & Applied Mathematics, University of Pretoria, Pretoria 0002, South Africa

Abstract

In this work, we consider numerical solutions of the FitzHugh-Nagumo system of equations describing the propagation of electrical signals in nerve axons. The system consists of two coupled equations: a nonlinear partial differential equation and a linear ordinary differential equation. We begin with a review of the qualitative properties of the nonlinear space independent system of equations. The sub equation approach is applied to derive dynamically consistent schemes for the sub models. This is followed by a consistent and systematic merging of the sub schemes to give three explicit nonstandard finite difference schemes in the limit of fast extinction and slow recovery. A qualitative study of the schemes together with the error analysis is presented. Numerical simulations are given to support the theoretical results and verify the efficiency of the proposed schemes.

Keywords: FitzHugh-Nagumo; Nonstandard finite difference; equilibrium point, kinematic model.
AMS Subject Classification: 65M06; 65M08; 65L12; 97N40

1 Introduction

The FitzHugh-Nagumo (FH-N) system is widely studied in applied mathematics, thanks to its rich dynamics, [15, 35, 20]. In this work we consider the FH-N system of equations in the form

$$\begin{aligned} \varepsilon \frac{du}{dt} &= f(u) - v + I \\ \frac{dv}{dt} &= u - \gamma v, \end{aligned} \tag{1.1}$$

where ε and γ are non negative constants. In addition, $f(u) = u(1-u)(u-\beta)$, where $\beta \in (0, \frac{1}{2})$. We are interested in the numerical discretisation of the equations in the limit case $\varepsilon \ll 1$, i.e., fast excitation and slow recovery [10, 18]. In the literature, the unknown u measures the potential difference across the cell membrane and the unknown v measures the transmembrane currents which influence the tendency of the cell to regain before being able to fire again. In addition, I is a

*Corresponding author. m.chapwanya@up.ac.za; Tel.: +27 12 420 2837; Fax.: +27 12 420 3893

constant stimulus which represents an externally applied current, [4]. The system of equations (1.1) is the simplified form of the Hodgkin-Huxley system used in the modeling of nerve axon dynamics. A non diffusive FH-N equation has been studied as a standard model for action potential of a nerve impulse, [14, 26]. It displays excitability which is also common in Hodgkins-Huxley and some other ionic models [19].

The theoretical and numerical analysis of the system of equations (1.1), and its reaction diffusion variants, have been studied extensively in the literature. Here we only highlight the results which are relevant for the current study. Results on existence of fast waves obtained using a geometric approach for singular perturbation problems can be found in [9]. On the other hand, results on the existence of traveling wave pulse for the reaction diffusion system for sufficiently small ε are reported in [8]. Further theoretical results have been reported by several other authors, see for example [28, 29, 30, 24].

Several numerical techniques have been developed to solve the FH-N system. Among these, is the variational iteration method (VIM) and the Adomian decomposition method (ADM) employed in [33]. The obtained results were compared with Hopscotch finite different scheme which was first proposed in [17], and further modified in [16]. Further simulations were obtained using the Galerkin-type schemes and collocation method and the results showed that only few terms are required to produce approximate solutions which are accurate and more efficient than the other schemes. It was also observed that the VIM is more accurate than the ADM. In [27], a pseudospectral method which is based on the use of Chebychev polynomials was shown to be useful in the study of the propagation of steep fronts.

It is also known that the use of standard time integration techniques such as forward or backward Euler and Runge-Kutta methods to solve such differential models often lead to numerical instabilities due to selection of discretisation parameters [13, 34, 22]. Despite the numerous application of nonstandard finite difference (NSFD) methods in approximating solutions of differential equations, it remains important to study the efficiency of these discretisation to the FH-N equations. In particular, NSFD schemes have the potential to be dynamically consistent with the properties of the continuous model. To the best of the authors knowledge, no work has been carried out on the use of NSFD discretisation for the system of the FH-N system of equations.

The idea of NSFD methods can be traced back to the work of Mickens in the late 1980's. A guiding philosophy in the construction of NSFD schemes is provided in [23]. Since then, significant progress has been made in the theory of these methods, see for example the contributions in [5]. The idea of the construction of the NSFD schemes is that the discrete model must preserve the properties of the continuous model they represent. Here we summarise some of the ideas for continuous dynamical systems.

Let $D \subset \mathbb{R}^d$ be a domain $(d \geq 1)$ and let $f \in C^0(D, \mathbb{R}^d)$ such that

$$\frac{dy}{dt} = f(y), \quad y(0) = y_0, \tag{1.2}$$

with $y_0 \in \mathbb{R}^d$ and $t > 0$. To introduce and develop the ideas of NSFD methods, we consider the ordinary differential equation (1.2). The numerical approximation of $y(t)$ is represented by y^n at time $t_n = n\Delta t$, where $n = 0, 1, \cdots$. An explicit finite difference scheme to (1.2) is expressed as follows

$$y^{n+1} = F(y^n; \Delta t), \quad y^0 = y_0. \tag{1.3}$$

Definition 1.1 ([5]). *A one-step scheme* (1.3) *is called a nonstandard finite difference scheme if at least one of the following conditions is satisfied:*

- *The classical denominator Δt, of the discrete derivative is replaced by a non-negative function $\phi(\Delta t)$ such that $\phi(\Delta t) = \Delta t + \mathcal{O}([\Delta t]^2)$;*
- *Nonlinear terms that occur in the right-hand side of* (1.2) *are approximated in a non-local way, e.g., $y^2 \approx y^n y^{n+1}$.*

The power and performance of the NSFD can be represented in terms of qualitative stability or dynamic consistency.

Definition 1.2 ([7]). *Assume the solution to a differential equation satisfies some property P. A numerical approximation* (1.3) *is dynamically consistent with the differential equation if the numerical solutions satisfy P for all values of the involved time step.*

Some of the properties highlighted in Definition 1.2 for equations in engineering and sciences include: positivity, boundedness, preservation of fixed-points and their stability properties, existence of special solutions (e.g., traveling waves, solitons, etc) and limit cycles and other periodic solutions. Since (1.2) is an autonomous differential equation, a stronger result on the solution for a one-dimensional problem is

Theorem 1.1 ([7]). *For $y \in \mathbb{R}$, the difference scheme* (1.3) *is qualitatively stable with respect to the monotonicity on initial values if and only if*

$$\frac{\partial F}{\partial v} \geq 0, \quad \Delta t > 0, \quad v \in \mathbb{R}.$$

The objective of this work is to present a systematic derivation of explicit nonstandard finite difference schemes for the FH-N model (1.1). A major property of the proposed NSFD schemes is that the discrete model preserves the properties of the continuous model, see Definition 1.2. Hence this work is motivated by the rich dynamics of the system (1.1) and its sub models, see for example [28, 29, 30, 24, 20] and references therein. In particular, we will only consider explicit schemes, and to keep the work focused, we only consider NSFD schemes.

This paper is organised as follows: in Section 2, we consider the temporal sub model of the system (1.1) and present its qualitative analysis. Here, three nonstandard finite difference schemes are presented for single-ODE equation and a system two-ODE equations of the FH-N equation. In each case, numerical experiments are performed to determine the performance of the schemes. In Section 3, we take motivation from Section 2 to derive schemes for the PDE models. In particular, schemes for the time and space independent equations are coupled to obtain complete schemes for the full system of FH-N equations. Numerical experiments are carried out for both the one-PDE-model and the system of FH-N equations. We end in Section 4 where conclusions and future directions are outlined.

2 The space independent FH-N model

We begin by presenting a qualitative study of the temporal model (1.1) for $I > 0$. The model is also identified in the literature as a FH-N model, see for example [20]. Many of the results discussed

here have been reported in [20, 4], and for completeness, we reformulate our requirements here. In the work, the authors showed the existence of both supercritical and subcritical bifurcations. A total of at least 8 bifurcation diagrams were observed. Here we are interested in the existence of equilibria for different selection of parameters. In particular, we have three distinct cases: one, two or three equilibria. Defining $\psi(u) = f(u) - u/\gamma$, so that $\psi(u) = -I$ at the equilibria, we have the following result.

Proposition 2.1 ([20]). *Let $E_e = (u_e, v_e)$ be an equilibrium point. If $\psi'(u_e) < 0$, then E_e is a stable node for $f'(u_e) < \gamma$ and is a repeller if $f'(u_e) > \gamma$. If $\psi'(u_e) > 0$, then E_e is a saddle point.*

The proof of this result follows directly from the Hartman-Grobman linearisation process. If γ and β are related by the inequality

$$\frac{1}{\gamma} > \frac{1}{3}\left(\beta - \frac{1}{2}\right)^2 + \frac{1}{4}, \tag{2.1}$$

the system of equations (1.1) has a unique equilibrium solution $E_0 = (u_0, v_0)$ which is asymptotically stable if $f'(u_0) < \gamma$ and $\psi'(u_0) < 0$. It is unstable if $f'(u_0) > \gamma$ and $\psi'(u_0) < 0$. The other cases can be discussed by defining

$$\delta := \frac{1}{3}\left(\beta - \frac{1}{2}\right)^2 + \frac{1}{4} - \frac{1}{\gamma}. \tag{2.2}$$

In this case, there exists one, two or three equilibria depending on the values of I. This scenario is shown in Figure 1 for a selection of parameters satisfying either $\delta < 0$ or $\delta > 0$. First we notice that Hopf bifurcation occurs when $\psi(u)$ has a minimum, $\psi(u_l) = -I_l$ and a maximum, $\psi(u_r) = -I_r$. If $I_r < -I$ and $I_l > -I$ there is only one equilibrium and $I = -I_r$ and $I = -I_l$ are saddle-node bifurcation values for I.

The three-equilibria case is obtained when $I_r < -I < I_r$. Here we identify the equilibria as follows: $E_0 = (u_0, v_0)$, $E_1 = (u_1, v_1)$ and $E_2 = (u_2, v_2)$ where $u_0 < u_1 < u_2$. E_1 is always a saddle point since $\psi'(u_1) > 0$, see Figure 1(b). If $\psi'(u_0) < 0$, $\psi'(u_2) < 0$ and $\gamma \geq 1$, then E_0 and E_2 are stable. Choosing a value $-\psi(u_2) > I$ and increasing I until $-\psi(u_1) < I$, only E_0 exists first and it is stable if I is very small. When the value of I is increased: E_0 becomes unstable; E_1 and E_2 show through a saddle-node bifurcation, E_2 showing instability; E_2 later becomes stable. These three processes show up but not always in this order. Eight different events are possible. For a complete discussion, see for example [20].

2.1 Numerical schemes

Throughout the paper, a numerical approximation of the unknown variable $w(x,t)$ on a uniform grid will be written as w_m^n at time $t_n = n\Delta t$ and spatial point $x_m = m\Delta x$, where $m = 0, 1, 2, \cdots, M$ and $n = 0, 1, 2, \cdots$. We begin by neglecting the equation for v in (1.1), i.e., we consider the FH-N equation given by

$$\varepsilon \frac{du}{dt} = f(u) = u(1-u)(u-\beta). \tag{2.3}$$

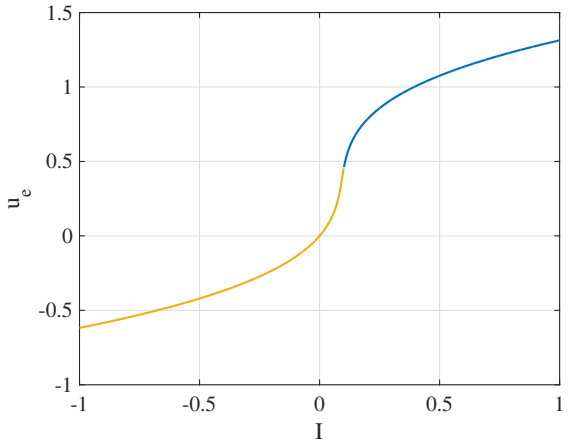

(a) Bifurcation diagram for $\delta < 0$.

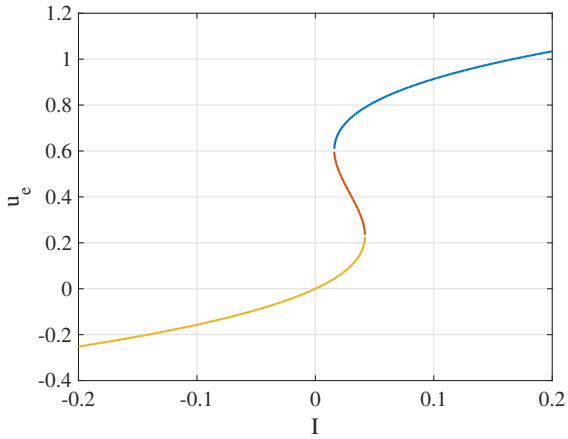

(b) Bifurcation diagram for $\delta > 0$.

Figure 1: Bifurcation diagram for the the FH-N system (1.1). In Figure (a) we choose $\beta = 0.139$, $\gamma = 2.54$, and in Figure (b) we have $\beta = 0.25$, $\gamma = 6.0$.

The three fixed points of equation (2.3) are $u_1^* = 0$, $u_2^* = 1$ and $u_3^* = \beta$. The fixed points u_1^* and u_2^* are both stable while u_3^* is unstable [31]. As pointed by [31], no effort will be made to find an exact scheme to (2.3) due to its complexity. We begin by recalling the following schemes (see [31, 32])

$$\varepsilon \frac{u^{n+1} - u^n}{\phi_1(\Delta t)} = -u^{n+1}(u^n)^2 + (1+\beta)(u^n)^2 - \beta u^{n+1}, \tag{2.4}$$

$$\varepsilon \frac{u^{n+1} - u^n}{\phi_1(\Delta t)} = -(2u^{n+1} - u^n)(u^n)^2 + (1+\beta)(u^n)^2 - \beta u^{n+1}, \tag{2.5}$$

where $\phi_1(\Delta t)$ is chosen to satisfy $\phi_1(\Delta t) = \Delta t + \mathscr{O}([\Delta t]^2)$. In particular, we have $\phi_1(\Delta t) = [\exp(\Delta t/\varepsilon) - 1]/(1/\varepsilon)$. These schemes preserve positivity and the stability/instability of the fixed points. Using a full nonlocal discretisation, we propose

$$\varepsilon \frac{u^{n+1} - u^n}{\phi(\Delta t)} = -u^{n+1}(u^n)^2 + (1+\beta)(u^n)u^{n+1} - \beta u^{n+1}, \tag{2.6}$$

where $\phi(\Delta t) = [1 - \exp(-\Delta t/\varepsilon)]/(1/\varepsilon)$. We notice that the right hand side of scheme (2.6) can be written in the form $u^{n+1}(1-u^n)(u^n - \beta)$ and it trivial to verify that the scheme preserves all the three fixed points. The numerical schemes (2.4), (2.5) and (2.6) can be written explicitly in the form

$$u^{n+1} = g(u^n), \tag{2.7}$$

for some function $g(u^n)$. We write scheme (2.6) explicitly as

$$u^{n+1} = g(u^n) = \frac{u^n}{1 + \phi\{(u^n)^2 - (1+\beta)u^n + \beta\}/\varepsilon}. \tag{2.8}$$

Clearly $g(u^n)|_{\Delta t=0} = u^n$. On differentiating $g(u^n)$, we have

$$g'(u^n) = \frac{1 + \phi\{\beta - (u^n)^2\}/\varepsilon}{\{1 + \phi[(u^n)^2 - (1+\beta)u^n + \beta]\}^2/\varepsilon}. \tag{2.9}$$

At fixed point u_1^*, we have

$$g'(0) = \frac{1}{1+\beta\phi/\varepsilon} \geq 0.$$

We also note that $|g'(0)| < 1$, hence the fixed point u_1^* is stable as expected. For the fixed point u_2^*, we have

$$g'(1) = 1 - \frac{\phi}{\varepsilon}(1-\beta) \geq 0,$$

using the definition of ϕ and the fact that $\beta \in (0, 1/2)$. In addition $|g'(1)| < 1$ so that u_2^* is also stable as expected. For the third fixed point u_2^*, we have

$$g'(\beta) = 1 + \beta\frac{\phi}{\varepsilon}(1-\beta) \geq 0,$$

since $\beta \in (0, 1/2)$. We also have $|g'(\beta)| > 1$ so that the fixed point u_3^* is unstable as expected. The above analysis prooves the following result.

Theorem 2.1. *The proposed new scheme* (2.6) *is topologically dynamically consistent with the properties of* (2.3)*.*

Remark 2.1. *We note that a similar analysis on the standard forward Euler scheme reveals that we need* $\Delta t < \dfrac{\varepsilon}{2\beta(1-\beta)}$ *to preserve the stability and monotonicity of initial values. That is,* Δt *is linearly dependent on* ε *which limits the efficiency of the scheme. In this work we aim to design schemes that remove this* $\varepsilon-$*dependence in the time stepping procedure, while keeping the algorithms as simple as possible.*

We test the performance of the presented schemes via an example as follows

Experiment 1. *Consider*

$$\begin{aligned} \varepsilon\frac{du}{dt} &= u(1-u)(u-\beta), \quad t > 0, \\ u(0) &= u_0. \end{aligned} \tag{2.10}$$

In Figure 2 we present simulations using schemes (2.4) – (2.6) to illustrate topological dynamic consistency of scheme (2.6). Comparison of nonstandard finite difference schemes with standard finite difference schemes is also provided elsewhere, see for example [3]. It is clear from Figure 2 that scheme (2.6) outperforms all the other schemes.

The above discussion and scheme (2.4)–(2.6), suggest that we have the following three possible schemes for the temporal system (1.1).

$$\begin{aligned} \varepsilon\frac{u^{n+1}-u^n}{\phi_1(\Delta t)} &= -u^{n+1}(u^n)^2 + (1+\beta)(u^n)^2 - \beta u^{n+1} - v^n + I, \\ \frac{v^{n+1}-v^n}{\phi_1(\Delta t)} &= u^n - \gamma v^n, \end{aligned} \tag{2.11}$$

$$\begin{aligned} \varepsilon\frac{u^{n+1}-u^n}{\phi_1(\Delta t)} &= -(2u^{n+1}-u^n)(u^n)^2 + (1+\beta)(u^n)^2 - \beta u^{n+1} - v^n + I, \\ \frac{v^{n+1}-v^n}{\phi_1(\Delta t)} &= u^n - \gamma v^n, \end{aligned} \tag{2.12}$$

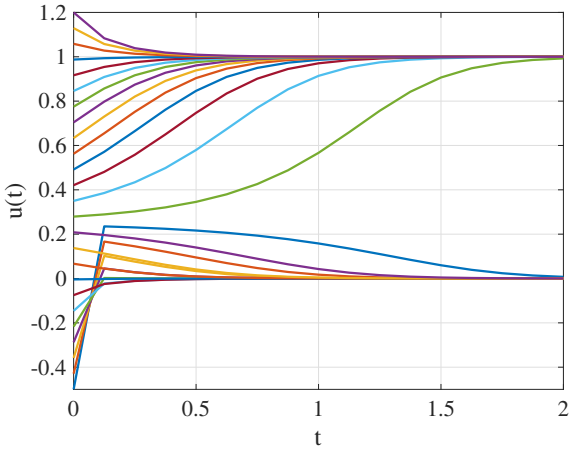

(a) Scheme (2.4).

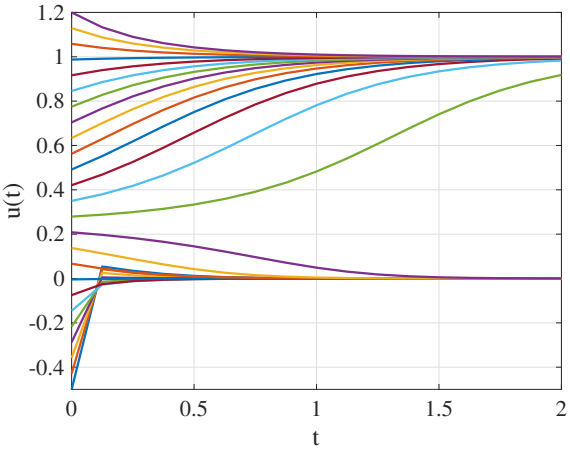

(b) Scheme (2.5).

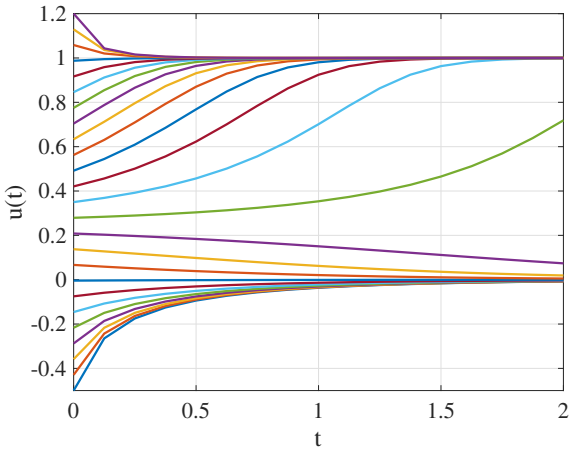

(a) Scheme (2.6).

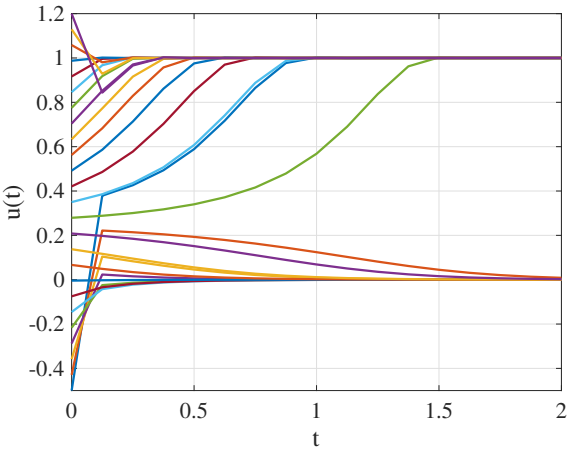

(b) Standard scheme.

Figure 2: In the simulations we choose $\beta = 0.25$ and $t_{\max} = 2$ for different initial values.

and

$$\begin{aligned} \varepsilon \frac{u^{n+1} - u^n}{\phi(\Delta t)} &= -u^{n+1}(u^n)^2 + (1+\beta)(u^n)u^{n+1} - \beta u^{n+1} - v^n + I, \\ \frac{v^{n+1} - v^n}{\phi(\Delta t)} &= u^n - \gamma v^n. \end{aligned} \tag{2.13}$$

For the purpose of comparison, we propose the following standard Euler scheme

$$\begin{aligned} \varepsilon \frac{u^{n+1} - u^n}{\Delta t} &= f(u^n) - v^n + I, \\ \frac{v^{n+1} - v^n}{\Delta t} &= u^n - \gamma v^n, \end{aligned} \tag{2.14}$$

where $f(u^n) = -(u^n)^3 + (1+\beta)(u^n)^2 - \beta u^n$. The analysis of the nonstandard schemes (2.11)-(2.13) is very complex and will not be presented here. However, we will use the following result which is based on the standard Euler scheme in benchmarking their performance.

Theorem 2.2. *Assuming that the function $f(u)$ satisfies the conditions $\gamma\varepsilon - f'(u_e) > 0$ and $1 - \gamma f'(u_e) > 0$, where (u_e, v_e) is the equilibrium point of system* (1.1)*, then the standard finite difference scheme* (2.14) *preserves the stability of the equilibrium (u_e, v_e) if*

$$\Delta t < \frac{\gamma\varepsilon - f'(u_e)}{1 - \gamma f'(u_e)}.$$

Remark 2.2. *In the literature, equations* (1.1)*,* (2.3) *and later on* (3.8) *have all been identified as FitzHugh-Nagumo equations. This also includes the reaction diffusion model to be considered later in the paper.*

2.2 Numerical simulations

In this section we perform numerical experiments of the system of equations (1.1) by choosing parameters so that they satisfy the existence and stability results summarised above. The examples considered here do not represent all the possible bifurcation scenarios for system (1.1). In particular, [20] gave eight possible scenarios and we are not going to simulate all of them here. The main purpose of this section is to show that the derived schemes preserve the properties of the continuous model. In all the experiments in this section, we consider

Experiment 2. *Consider model* (1.1) *subject to initial conditions, $u(0) = u_0$, and $v(0) = v_0$.*

The selection of parameters will be explained in the text.

2.2.1 Single equilibrium

We first consider the case where there exists one equilibrium, in which case the relation given by equation (2.1) must be satisfied. Here we choose $\beta = 0.139$, $\gamma = 2.54$ and $\varepsilon = 0.008$, as used in [4], and a single equilibrium point E_0 is obtained. The corresponding bifurcation diagram is given in Figure 1.

From Proposition 2.1, it is found that for $I = 0.026$, $E_0 = (0.0546, 0.0215)$ is a stable equilibrium and for $I = 0.05$, $E_0 = (0.1225, 0.04823)$ is an unstable equilibrium. The two cases are illustrated by plotting phase trajectories as given in Figures 3. To test the performance of the schemes, we select $\Delta t = 0.01$ which is within the stability restriction for standard forward scheme as summarised in Theorem 2.2, and $\Delta t = 0.1$ for NSFD schemes. In particular, for the selection of parameters here, the forward Euler scheme requires that $\Delta t < 0.0408$. While it is clear from the figures that schemes (2.11), (2.12) and (2.14) develop nonphysical oscillations over time, scheme (2.13) provides spurious free simulations.

In Figure 4, we illustrate further the stability of the equilibrium for different initial values using scheme (2.13) alone and $\Delta t = 0.1$. The results support the local stability given in Proposition 2.1.

2.2.2 More than one equilibrium

The simulations in this section are motivated by the authors in [20], where some arguments were given with respect to the convergence of trajectories to either of the equilibrium points for a given

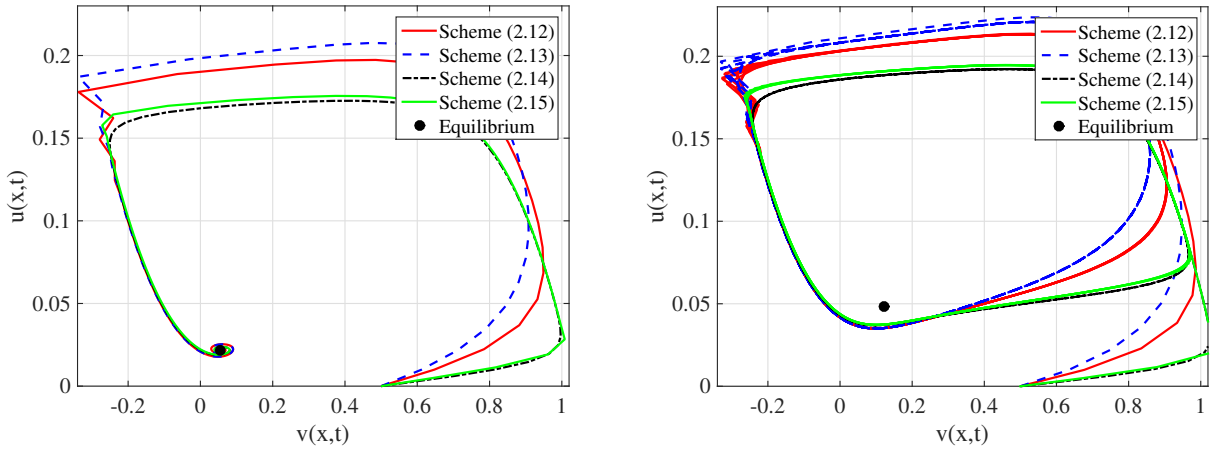

(a) E_0 is stable. (b) E_0 is unstable.

Figure 3: Phase plane trajectories in the (u, v) plane when: (a) E_0 is stable, and (b) E_0 is unstable.

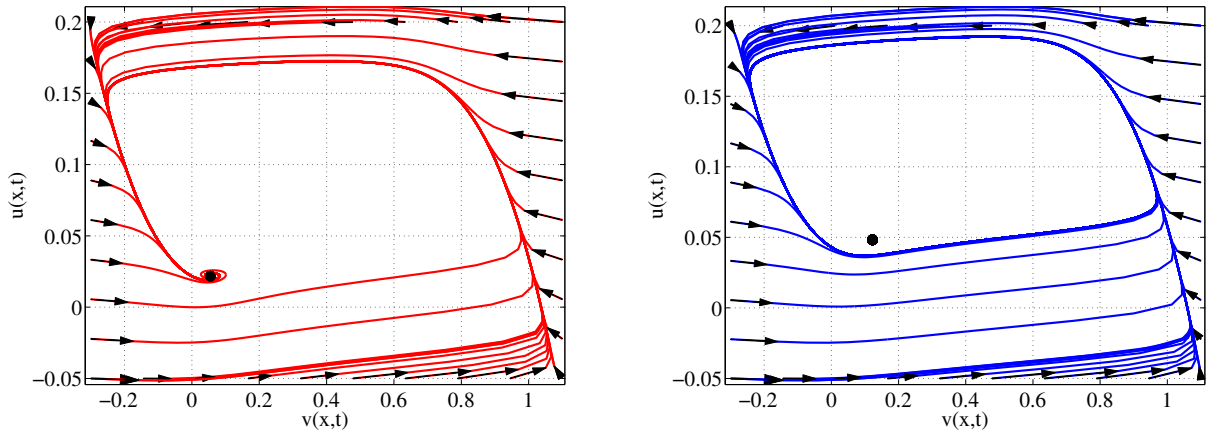

(a) E_0 is stable. (b) E_0 is unstable.

Figure 4: Phase plane trajectories in the (u, v) plane when: (a) E_0 is stable, and (b) E_0 is unstable.

initial condition. For this case of more than one equilibrium, we choose the parameter β, γ such that relation $\delta > 0$ given above holds. In particular, we choose $\beta = 0.25, \gamma = 6, \varepsilon = 0.01$ and $I = 0.035$ so that model (1.1) is bistable. We obtain the three equilibria given by $E_0 = (0.1283, 0.0214)$, $E_1 = (0.3563, 0.0594)$ and $E_2 = (0.7653, 0.1276)$.

We give convergence results in Figures 5 – 8 where for each scheme we choose $\Delta t = 0.03$ and $\Delta t = 0.003$. While scheme (2.13) shows converged results at $\Delta t = 0.03$, the other three schemes need a much smaller time step for the trajectories to be attracted to the correct equilibrium.

3 The spatial models

Following earlier work on NSFD methods, a natural approach will be to derive schemes for the sub equations and then merge them to design a scheme for the full equation, c.f. [23, 11]. Here we

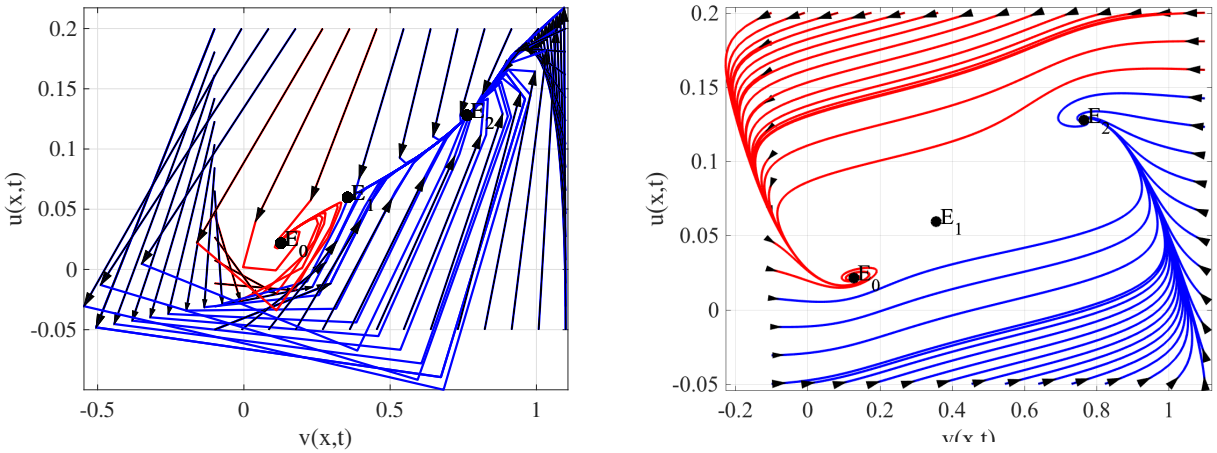

(a) $\Delta t = 0.03$. (b) $\Delta t = 0.003$.

Figure 5: Phase plane trajectories in the (u, v) plane when: E_0 and E_2 are stable with E_1 unstable, using scheme (2.11).

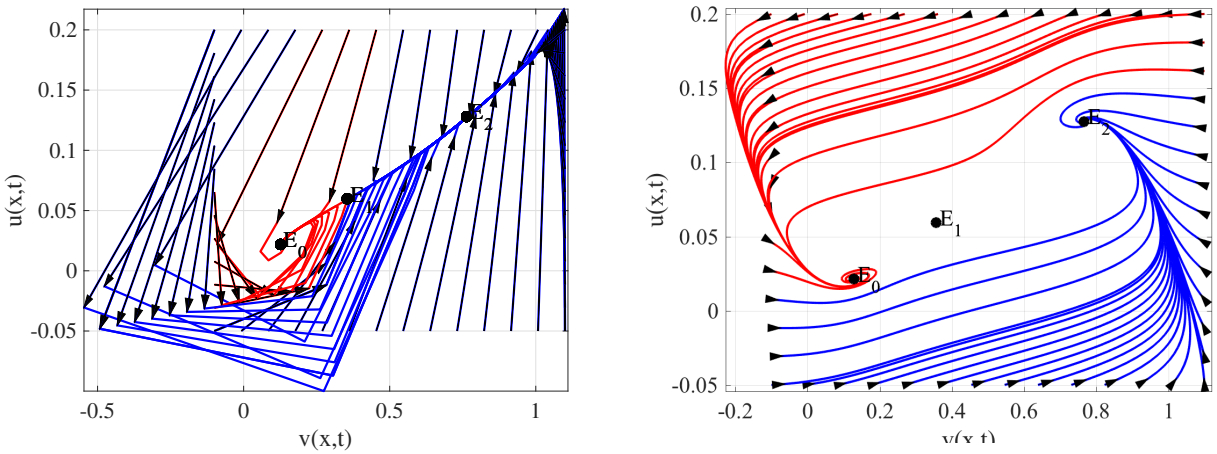

(a) $\Delta t = 0.03$. (b) $\Delta t = 0.003$.

Figure 6: Phase plane trajectories in the (u, v) plane when: E_0 and E_2 are stable with E_1 unstable, using scheme (2.12).

follow the same approach to design NSFD schemes for the following model

$$\begin{aligned} \varepsilon \frac{\partial u}{\partial t} &= \varepsilon \frac{\partial^2 u}{\partial x^2} + f(u) - v + I \\ \frac{\partial v}{\partial t} &= u - \gamma v, \end{aligned} \tag{3.1}$$

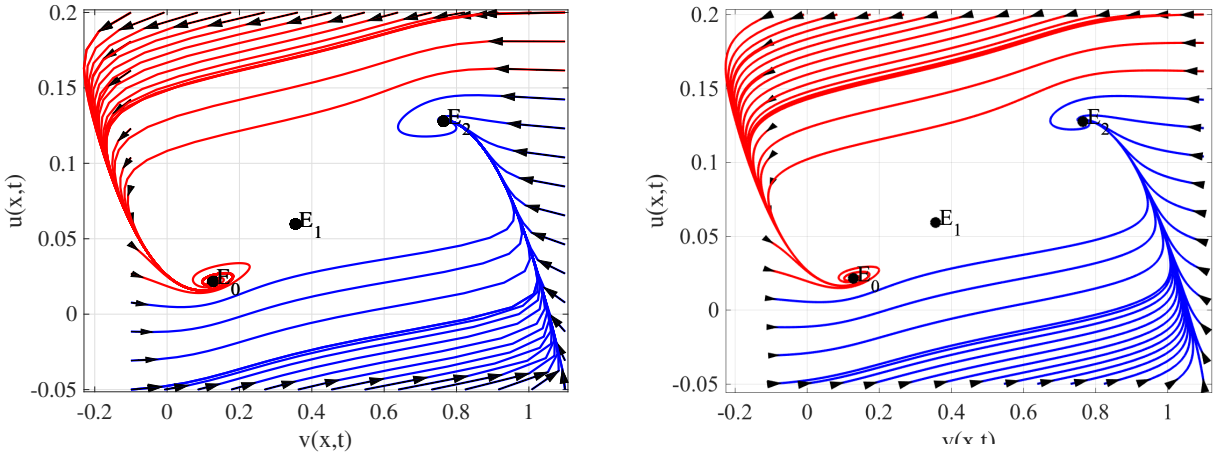

(a) $\Delta t = 0.03$. (b) $\Delta t = 0.003$.

Figure 7: Phase plane trajectories in the (u, v) plane when: E_0 and E_2 are stable with E_1 unstable, using scheme (2.13).

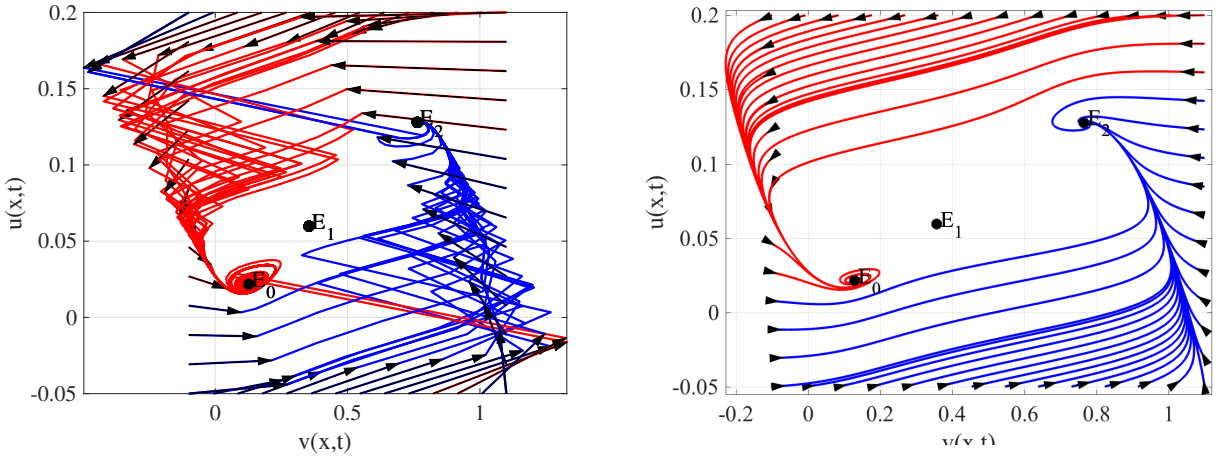

(a) $\Delta t = 0.03$. (b) $\Delta t = 0.003$.

Figure 8: Phase plane trajectories in the (u, v) plane when: E_0 and E_2 are stable with E_1 unstable, using scheme (2.14).

where $x \in \Omega$. First we consider the time independent problem for (3.1) given by

$$\begin{aligned} \varepsilon \frac{\partial^2 u}{\partial x^2} + f(u) - v + I &= 0 \\ u - \gamma v &= 0. \end{aligned} \tag{3.2}$$

The second equation simplifies to $v = u/\gamma$, and therefore we have

$$\varepsilon \frac{\partial^2 u}{\partial x^2} - u^3 + (1+\beta)u^2 - \beta u - \frac{u}{\gamma} + I = 0. \tag{3.3}$$

The equation depicts the steady state reaction diffusion equation which has been studied extensively in the literature, see for example [4, 27, 12]. A first integral of (3.3) is

$$E = \frac{\varepsilon}{2}\left(\frac{\partial u}{\partial x}\right)^2 - \frac{u^4}{4} + (1+\beta)\frac{u^3}{3} - \beta\frac{u^2}{2} - \frac{1}{\gamma}\frac{u^2}{2} + uI, \tag{3.4}$$

where E is a constant representing the energy, see [6]. A corresponding discrete energy preserving form is,

$$\frac{\varepsilon}{2}\left(\frac{u_{m+1}-u_m}{\psi(\Delta x)}\right)^2 + G(u_m u_{m+1}) = \frac{\varepsilon}{2}\left(\frac{u_m-u_{m-1}}{\psi(\Delta x)}\right)^2 + G(u_m u_{m-1}), \tag{3.5}$$

which is invariant under the transformation $m \leftrightarrow m+1$, with $\psi(\Delta x)$ satisfying $\psi(\Delta x) = \Delta x + \mathcal{O}([\Delta x]^2)$. The exact scheme is

$$\varepsilon\frac{u_{m+1}-2u_m+u_{m-1}}{\psi(\Delta x)^2} - u_m^2\left(\frac{u_{m+1}+u_{m-1}}{2}\right) + (1+\beta)u_m\left(\frac{u_{m+1}+u_m+u_{m-1}}{3}\right) - \beta u_m - \frac{u_m}{\gamma} + I = 0. \tag{3.6}$$

Consequently, we propose the following scheme for (3.2),

$$\varepsilon\frac{u_{m+1}-2u_m+u_{m-1}}{\psi(\Delta x)^2} - u_m^2\left(\frac{u_{m+1}+u_{m-1}}{2}\right) + (1+\beta)u_m\left(\frac{u_{m+1}+u_m+u_{m-1}}{3}\right) - v_m + I = 0, \tag{3.7}$$

$$u_m - \gamma v_m = 0.$$

In the next sections, the scheme derived above will be combined with the schemes for the temporal model derived in Section 2 and numerical simulations will be performed to test their performance.

3.1 Single FH-N equation

As highlighted above, there are several variants of the FH-N equations. A single FH-N equation as formulated in Experiment 3 is often referred to as the FH-N model, see [21, 2]

Experiment 3. *Consider*

$$\begin{aligned} \varepsilon\frac{\partial u}{\partial t} &= \varepsilon\frac{\partial^2 u}{\partial x^2} + u(1-u)(u-\beta), \quad x \in (\infty,\infty) \\ u(x,0) &= w(x,0), \\ \lim_{x\to-\infty} u(x,t) = 1, &\quad \lim_{x\to-\infty} u(x,t) = 0, \end{aligned} \tag{3.8}$$

where $w(x,t)$ is the travelling wave solution given in [21], i.e.,

$$w(x,t) = \frac{1}{2} - \frac{1}{2}\tanh\left\{\frac{x-ct}{2\sqrt{2}}\right\}.$$

The traveling wave speed is $c = \sqrt{2}(1-2\beta)/2\varepsilon$.

The following schemes will be considered: combining schemes (2.4) and (3.7) gives

$$\varepsilon\frac{u_m^{n+1}-u_m^n}{\phi_1(\Delta t)}=\varepsilon\frac{u_{m+1}^n-2u_m^n+u_{m-1}^n}{[\psi(\Delta x)]^2}-u_m^n u_m^{n+1}\left(\frac{u_{m+1}^n+u_{m-1}^n}{2}\right)+(1+\beta)u_m^n\left(\frac{u_{m+1}^n+u_m^n+u_{m-1}^n}{3}\right)-\beta u_m^{n+1}, \quad (3.9)$$

combining schemes (2.5) and (3.7) gives

$$\varepsilon\frac{u_m^{n+1}-u_m^n}{\phi_1(\Delta t)}=\varepsilon\frac{u_{m+1}^n-2u_m^n+u_{m-1}^n}{[\psi(\Delta x)]^2}-(2u_m^{n+1}-u_m^n)u_m^n\left(\frac{u_{m+1}^n+u_{m-1}^n}{2}\right)+(1+\beta)u_m^n\left(\frac{u_{m+1}^n+u_m^n+u_{m-1}^n}{3}\right)-\beta u_m^{n+1}, \quad (3.10)$$

and finally, combining schemes (2.6) and (3.7) gives

$$\varepsilon\frac{u_m^{n+1}-u_m^n}{\phi(\Delta t)}=\varepsilon\frac{u_{m+1}^n-2u_m^n+u_{m-1}^n}{[\psi(\Delta x)]^2}-u_m^n u_m^{n+1}\left(\frac{u_{m+1}^n+u_{m-1}^n}{2}\right)+(1+\beta)u_m^{n+1}\left(\frac{u_{m+1}^n+u_m^n+u_{m-1}^n}{3}\right)-\beta u_m^{n+1}. \quad (3.11)$$

We present profiles of the solutions for different selection of ε in Figure 9. The L_∞ errors for all the schemes for different values of the number of grid points in space, is plotted in Figure 10. In all the simulations we use

$$R=\frac{\phi(\Delta t)}{\psi^2(\Delta x)}=\frac{1}{2}.$$

From Figure 10, it is seen that scheme (3.11) produces the least error followed by scheme (3.10). It is clear that all profiles for schemes (3.9) – (3.11) are almost indistinguishable with the exact solution.

3.2 System of FH-N equations

In this section we consider nonstandard finite difference schemes for the full system of equations given in (3.1). The system represent a coupled differential system in activator-inhibitor variables. We will study the convergence of two different schemes whose derivation was motivated by the preceding sections. A traveling wave problem derived from (3.1) with $I = 0$ was investigated in [25]. The asymptotic traveling wave speed was obtained to be

$$c=\frac{1-2\beta}{\sqrt{2\varepsilon}},$$

defined using the current variables. Convergent numerical solutions, with respect to the traveling wave speed, are given in [27]. In their work, pseudospectral methods were used and the exact wave speed was compared with the numerical approximations. We will adopt their numerical experiment to show that the proposed nonstandard finite difference method is also efficient for non smooth problems that develop shock-like steep fronts.

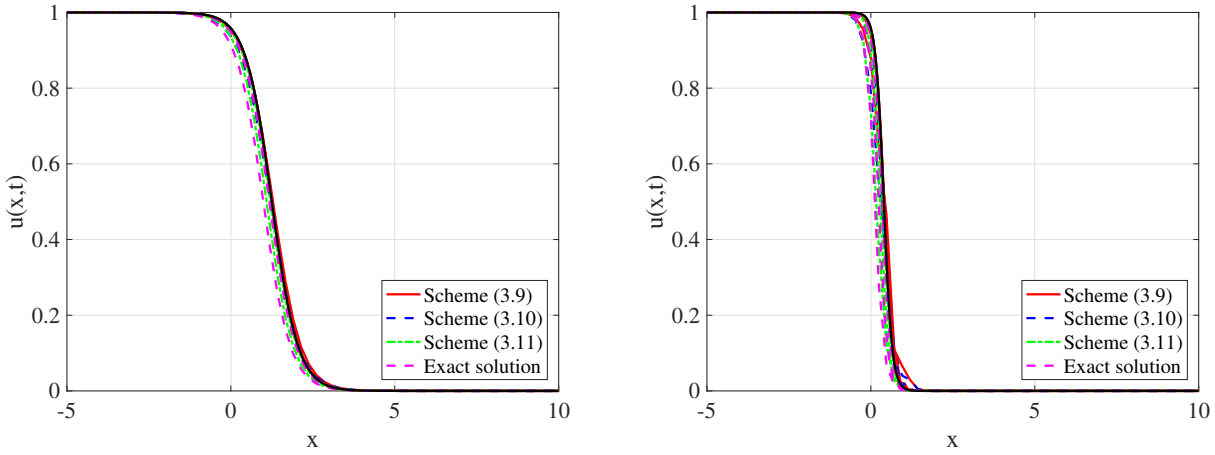

(a) $\varepsilon = 0.08$. (b) $\varepsilon = 0.008$.

Figure 9: Profiles for the travelling wave solution with comparison to the exact solution. We choose $\beta = 0.25$, $t_{\max} = 1$, $M = 64$ and a truncated domain $x \in (-5, 15)$.

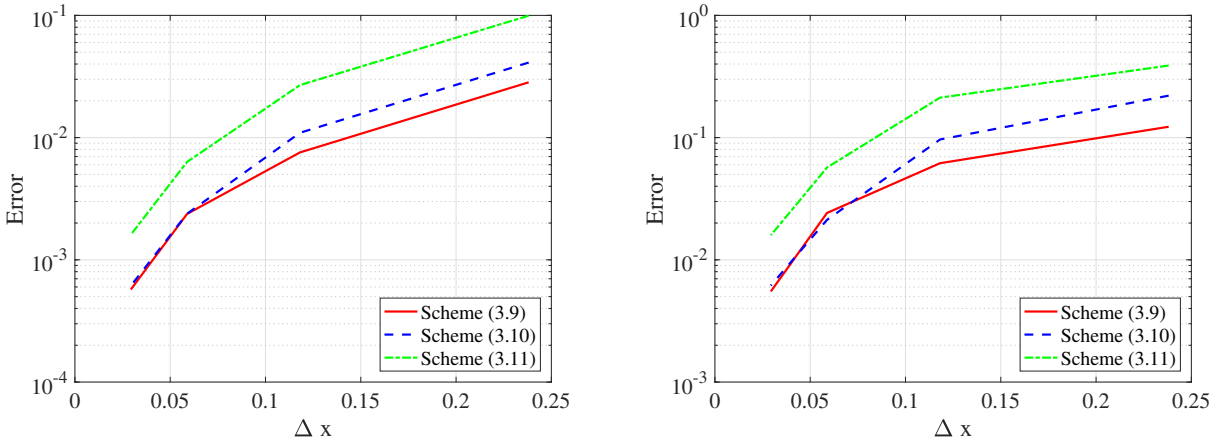

(a) $\varepsilon = 0.08$. (b) $\varepsilon = 0.008$.

Figure 10: L_∞ error plots for the four schemes. We choose $\beta = 0.25$, $t_{\max} = 1$ and a truncated domain $x \in (-5, 15)$.

Combining schemes (2.11) and (3.7), we have

$$\varepsilon \frac{u_m^{n+1} - u_m^n}{\phi_1(\Delta t)} = \varepsilon \frac{u_{m+1}^n - 2u_m^n + u_{m-1}^n}{\psi^2(\Delta x)} - u_m^n u_m^{n+1} \left(\frac{u_{m+1}^n + u_{m-1}^n}{2} \right) + (1+\beta) u_m^n \left(\frac{u_{m+1}^n + u_m^n + u_{m-1}^n}{3} \right) - \beta u_m^{n+1} - v_m^n + I, \quad (3.12)$$

$$\frac{v_m^{n+1} - v_m^n}{\phi_1(\Delta t)} = u_m^n - \gamma v_m^n,$$

and combining schemes (2.13) and (3.7), we have

$$\varepsilon\frac{u_m^{n+1}-u_m^n}{\phi(\Delta t)} = \varepsilon\frac{u_{m+1}^n-2u_m^n+u_{m-1}^n}{\psi^2(\Delta x)} - u_m^n u_m^{n+1}\left(\frac{u_{m+1}^n+u_{m-1}^n}{2}\right)+$$
$$(1+\beta)u_m^{n+1}\left(\frac{u_{m+1}^n+u_m^n+u_{m-1}^n}{3}\right) - \beta u_m^{n+1} - v_m^n + I, \quad (3.13)$$
$$\frac{v_m^{n+1}-v_m^n}{\phi(\Delta t)} = u_m^n - \gamma v_m^n.$$

We test the performance of these schemes by considering several experiments. In the first experiment we have

Experiment 4. *We solve system* (3.1) *subject to periodic boundary conditions and*

$$u(x,0) = 0.5, \quad v(x,0) = 0. \quad (3.14)$$

The parameters are chosen following Experiment 2, i.e., $\beta = 0.139$, $\gamma = 2.54$ *and* $\varepsilon = 0.008$. *In addition,* $I = 0.026$ *for a single and stable equilibrium, and* $I = 0.05$ *for a single and unstable equilibrium with respect to ODE model* (3.1).

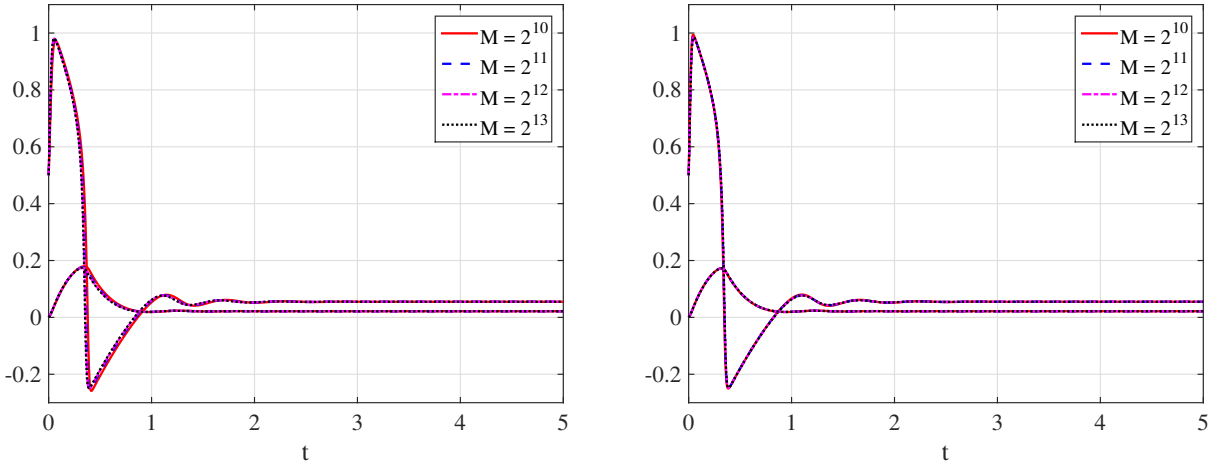

(a) Scheme (3.12). (b) Scheme (3.13).

Figure 11: Convergence results corresponding to Experiment 4 for $I = 0.026$ and $R = 0.4$.

In Figures 11 and 12 we display solution profiles of $u(x^*,t)$ and $v(x^*,t)$ against t on the same axes for $x^* = 5$. In each figure, we run simulations for different number of temporal grid points. While simulations in Figure 11 show comparable convergence for the two schemes, the case is different in Figure 12. Here scheme (3.13) is more superior compared to scheme (3.12).

The next experiment is motivated by the work of [27].

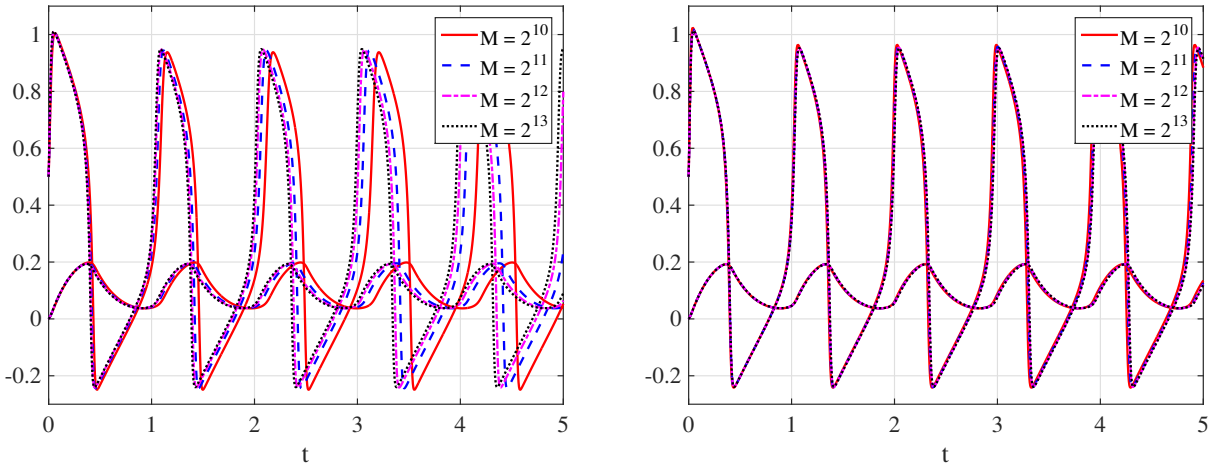

(a) Scheme (3.12). (b) Scheme (3.13).

Figure 12: Convergence results corresponding to Experiment 4 for $I = 0.05$ and $R = 0.4$.

Experiment 5. *We solve system* (3.1) *subject to zero-flux boundary conditions and*

$$u(x,0) = \begin{cases} 0 & x > 0 \\ u_0(x) & \textit{otherwise} \end{cases}, \quad v(x,0) = \begin{cases} 0.15 & x < -17 \\ 0 & \textit{otherwise} \end{cases}. \tag{3.15}$$

where $\beta = 0.1$, $\gamma = 0.5$, $\varepsilon = 0.001$, $I = 0$ *and*

$$u_0(x) = \frac{1}{(1+\exp(4|x|-17))^2} - \frac{1}{(1+\exp(4|x|-13))^2}.$$

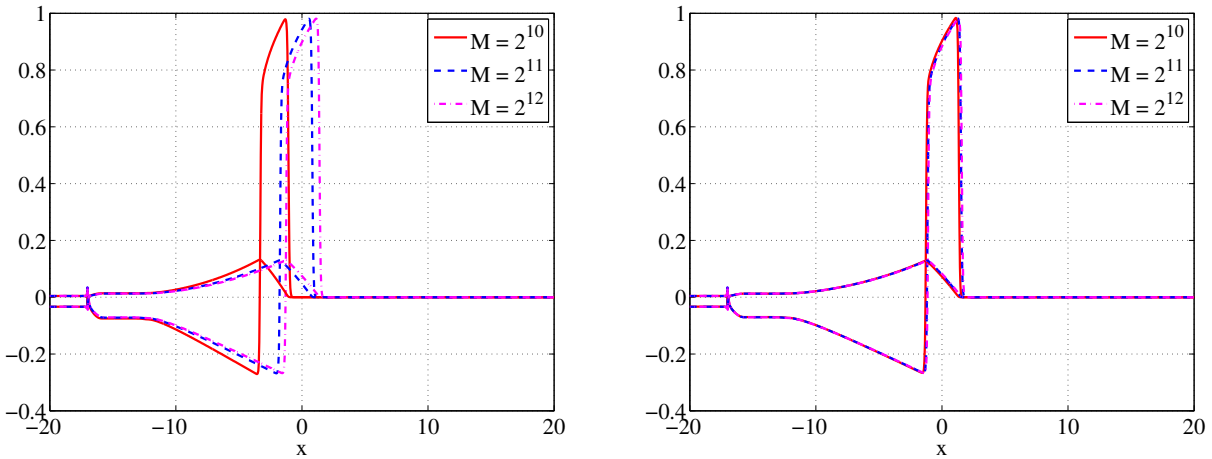

(a) Scheme (3.12). (b) Scheme (3.13).

Figure 13: Convergence results for Experiment 5 with different choices of spatial grid spacing and $R = 0.4$.

Convergence results for different choices of spatial grid spacing are given in Figure 13 for $u(x,t^*)$ and $v(x,t^*)$ with $t^* = 1.0$. The rapid convergence of scheme (3.13) is evident. In particular, for the chosen grid spacing, the solution profiles are indistinguishable.

4 Conclusion

The purpose of this work was to design explicit nonstandard finite difference schemes for the FH-N system of equations in the limit $\varepsilon \to 0$. The work is motivated by earlier literature where NSFD methods were found to be efficient in cases where oscillatory solutions or problems that develop shock-like steep fronts are investigated, [1]. In addition, the rich dynamics of the temporal model presented in [20] motivates the idea of efficient discrete models for the system. In particular, existence of multiple equilibria and rich bifurcation events (based on the stimuli I), makes any numerical approach for such a system of equations complicated.

We presented nonstandard finite difference schemes for the FH-N system of reaction diffusion equations. Four different sub models of the full FH-N system were considered: the temporal single ODE model, the temporal system, the single PDE model and the full reaction diffusion system. We started by recalling the qualitative analysis of the temporal model with the aim to design schemes preserving the properties of this continuous model. Three explicit schemes were proposed and their performances was benchmarked against a standard explicit finite difference scheme. Our results showed the superiority of NSFD schemes and spurious-oscillation-free simulations were observed.

Acknowledgements

The authors acknowledge the support of South African DST/NRF SARChI Chair on Mathematical Models and Methods in Bioengineering and Biosciences (M^3B^2) of the University of Pretoria. MC and AR also acknowledge the support of National Research Foundation of South Africa Grant Numbers 93476 and 95864 respectively. Thanks are also addressed to the anonymous reviewers whose suggestions have contributed to the improvement of the paper.

References

[1] A.A. Aderogba, M. Chapwanya, J. Djoko Kamdem, and J.M.-S. Lubuma. *Coupling finite volume and nonstandard finite difference schemes for a singularly perturbed Schrödinger equation,* Int. J. Comput. Math., 93 (2016), pp. 1833–1844.

[2] A.A. Aderogba, M. Chapwanya, and O.A. Jejeniwa. *Finite difference discretisation of a model for biological nerve conduction,* In International Conference of Numerical Analysis and Applied Mathematics 2015 (ICNAAM 2015), volume 1738, page 030009. AIP Publishing.

[3] A.A. Aderogba and M. Chapwanya. *An explicit nonstandard finite difference scheme for the Allen–Cahn equation,* J. Difference Equ. Appl., 21 (2015), pp. 875–886.

[4] J.G. Alford and G. Auchmuty. *Rotating wave solutions of the FitzHugh–Nagumo equations,* J. Math. Biol., 53 (2006), pp. 797–819.

[5] R. Anguelov and J.M-S. Lubuma. *Contributions to the mathematics of the nonstandard finite difference method and applications,* Numer. Methods Partial Differential Equations, 17 (2001), pp. 518–543.

[6] R. Anguelov, P. Kama, and J.M-S. Lubuma. *On non-standard finite difference models of reaction–diffusion equations,* J. Comput. Appl. Math., 175 (2005), pp. 11–29.

[7] R. Anguelov and J.M.-S. Lubuma. *Nonstandard finite difference method by nonlocal approximation,* Math. Comput. Simulation, 61 (2003), pp. 465–475.

[8] G. Arioli and H. Koch. *Existence and stability of traveling pulse solutions of the FitzHugh–Nagumo equation,* Nonlinear Anal., 113 (2015), pp. 51–70.

[9] G.A. Carpenter. *A geometric approach to singular perturbation problems with applications to nerve impulse equations,* J. Differential Equations, 23 (1977), pp. 335–367.

[10] A. Carpio and L.L. Bonilla. *Pulse propagation in discrete systems of coupled excitable cells,* SIAM J. Appl. Math., 63 (2003), pp. 619–635.

[11] M. Chapwanya, J.M.-S. Lubuma, and R.E. Mickens. *Nonstandard finite difference schemes for Michaelis–Menten type reaction-diffusion equations,* Numer. Methods Partial Differential Equations, 29 (2013), pp. 337–360.

[12] M. Chapwanya, J.M.-S. Lubuma, and R.E. Mickens. *From enzyme kinetics to epidemiological models with Michaelis–Menten contact rate: Design of nonstandard finite difference schemes,* Comput. Math. Appl., 64 (2012), pp. 201–213.

[13] Z. Chen, A.B. Gumel, and R.E. Mickens. *Nonstandard discretizations of the generalized Nagumo reaction-diffusion equation,* Numer. Methods Partial Differential Equations, 19 (2003), pp. 363–379.

[14] R. FitzHugh. *Impulses and physiological states in theoretical models of nerve membrane,* Biophys. J., 1 (1961), pp. 445–466.

[15] C. Rocsoreanu, A. Georgescu and N. Giurgiteanu. *The FitzHugh-Nagumo model: bifurcation and dynamics*, Mathematical modelling: theory and applications, volume 10. Springer-Science + Business Media, B.V., Kluwer Academic, New York, (2000)

[16] A.R. Gourlay. *Hopscotch: a fast second-order partial differential equation solver,* IMA J. Appl. Math., 6 (1970), pp. 375–390.

[17] P. Gordon. *Nonsymmetric difference equations,* Journal of the Society for Industrial and Applied Mathematics, 13 (1965), pp. 667–673.

[18] J. Guckenheimer and C. Kuehn. *Homoclinic orbits of the FitzHugh–Nagumo equation: Bifurcations in the full system,* SIAM J. Appl. Dyn. Syst., 9 (2010), pp.138–153.

[19] J.P. Keener and J. Sneyd. *Mathematical physiology*, volume 1. New York: Springer, 1998.

[20] T. Kostova, R. Ravindran, and M. Schonbek. *Fitzhugh–Nagumo revisited: Types of bifurcations, periodical forcing and stability regions by a Lyapunov functional,* Int. J. Bifurc. Chaos, 14 (2004), pp. 913–925.

[21] Y.N. Kyrychko, M.V. Bartuccelli, and K.B. Blyuss. *Persistence of travelling wave solutions of a fourth order diffusion system,* J. Comput. Appl. Math., 176 (2005), pp. 433–443.

[22] R.E. Mickens. *Nonstandard finite difference schemes for reaction-diffusion equations,* Numer. Methods Partial Differential Equations, 15 (1999), pp. 201–214.

[23] R.E. Mickens. *Nonstandard finite difference models of differential equations*. World Scientific, Singapore, 1994.

[24] S. Mischler, C. Quininao and J. Touboul. *On a kinetic FitzHugh–Nagumo model of neuronal network,* Comm. Math. Phys., 342 (2016), pp.1001–1042.

[25] J.D. Murray. *Mathematical Biology II: Spatial Models and Biomedical Applications,* Interdisciplinary Applied Mathematics. Springer New York, 2011.

[26] J. Nagumo, S. Arimoto and S. Yoshizawa. *An active pulse transmission line simulating nerve axon.* Proceedings of the IRE, 50 (1962), pp. 2061–2070.

[27] D. Olmos and B.D. Shizgal. *Pseudospectral method of solution of the FitzHugh–Nagumo equation,* Math. Comput. Simulation, 79 (2009), pp. 2258–2278.

[28] J. Rauch and J. Smoller. *Qualitative theory of the FitzHugh-Nagumo equations,* Adv. Math., 27 (1978), pp.12–44.

[29] C. Reinecke and G. Sweers. *Existence and uniqueness of solutions on bounded domains to a FitzHugh–Nagumo type elliptic system,* Pacific J. Math., 197 (2001), pp. 183–211.

[30] C. Reinecke and G. Sweers. *Solutions with internal jump for an autonomous elliptic system of FitzHugh–Nagumo type,* Math. Nachr., 251 (2003), pp. 64–87.

[31] L-I.W. Roeger and R.E Mickens. *Exact finite-difference schemes for first order differential equations having three distinct fixed-points.* J. Difference Equ. Appl., 13 (2007), pp. 1179–1185.

[32] L-I.W. Roeger. *Nonstandard finite difference schemes for differential equations with n+1 distinct fixed-points,* J. Difference Equ. Appl., 15 (2009), pp. 133–151.

[33] A.A. Soliman. *Numerical simulation of the FitzHugh-Nagumo equations,* Abstr. Appl. Anal., 2012 (2012), ID 762516.

[34] E.H. Twizell, A.B. Gumel. and Q. Cao. *A second-order scheme for the Brusselator reaction–diffusion system,* J. Math. Chem., 26 (1999), pp. 297–316.

[35] B. Zinner. *Existence of traveling wavefront solutions for the discrete Nagumo equation,* J. Differential Equations, 96 (1992), pp. 1–27.